J. Cent. South Univ. (2015) 22: 2119−2126
DOI: 10.1007/s11771-015-2736-y

Springer

Geometric design and simulation of tooth profile using elliptical segments as its line of action

WANG Jian(王建)[1, 2], LUO Shan-ming(罗善明)[1, 2], SU De-yu(苏德瑜)[2, 3], CHANG Xue-feng(常雪峰)[1, 2]

1. School of Mechanical & Automotive Engineering, Xiamen University of Technology, Xiamen 361024, China;
2. Key Laboratory of Precision Actuation and Transmission of Fujian Province University, Xiamen 361024, China;
3. School of Electromechanical Engineering, Hunan University of Science and Technology, Xiangtan 411201, China

© Central South University Press and Springer-Verlag Berlin Heidelberg 2015

Abstract: A mathematical model of gear tooth profiles using the ellipse curve, whose curvature is convenient to control by changing the mathematical parameters as its line of action, was built based on the meshing theory. The equation of undercutting condition was derived from the model. A special epicycloidal tooth profile was also presented. An example gear drive with variation of the ellipse parameters was taken to illustrate the proposed method. The contact ratio of the gear drive designed by the proposed method was analyzed. A comparison of the property of the gear drive designed with the involute gear drive was also carried out. The results confirm that the proposed gear drive has higher contact ratio in comparison with the involute gear drive.

Key words: gear transmission; tooth profile; elliptical segment; epicycloidal; contact ratio

1 Introduction

Gears are widely applied in industry and in common life. In different situations gears are used for different purposes. For instance, a gear box in a car is used for power transmission. Gears in a hard disk are used to transmit movement from a stepper motor to the magnetic head in order to read the data stored in a specific track on the disk. Gears are also used in a gear pump to transfer liquid from one place to another. The different circumstances of gears application affect the design of the profiles. The development of new tooth profiles has been the subject of intensive research in Refs. [1−5]. But the current design technique for gears is confined to several types of tooth surface form. An active design method for special tooth profiles has also been proposed recently [6−10], but it has not been formed a complete system.

Most kinematical characteristics of a spur gear drive can be determined by the line of action (i.e., the summation of instant contact points in the fixed coordinate system). Several studies have been focused on the active design method based on the line of action. CAO et al [11] presented a new design method for spiral bevel gears on the basis of meeting the contact conditions inclusive of the pre-designed parabolic function of transmission errors and the specifically oriented straight contact path through three given control points on the tooth surface. TSAI and HSU [12] introduced a method to design spiral bevel gear sets with circular-arc contact paths. FONG et al [13] illustrated the mathematical model with an example of a combinative curve that comprises a straight line and a circular arc. WANG et al [14] introduced a method for design of gear tooth profiles using parabolic curve as its line of action. This work offers a method to design tooth profiles using elliptical segments as the line of action. The mathematical model of spur gears using elliptical segments as the line of action is provided. An example gear drive using the proposed design method is carried out.

2 Geometrical modeling of tooth profiles based on line of action

As shown in Fig. 1, coordinate systems Σ_1 and Σ_2 are moving coordinate systems rigidly connected to the driving gear and the driven gear, respectively; while coordinate system Σ_0 is a fixed coordinate system. Points O_1 and O_2 are the centers of the driving and the driven gears, respectively; while point O_0 lies at the intersection of the x_0-axis and y_0-axis. Point P is the pitch point,

Foundation item: Projects(51205335, 51375411) supported by the National Natural Science Foundation of China; Projects(2013J01209, 2012J01237) supported by the Natural Science Foundation of Fujian Province, China; Project(2014H0049) supported by the Major S&T Program of Fujian Province, China; Project(E201400800) supported by the International Cooperation and Exchange Research Plan of Xiamen University of Technology, China; Project(YKJ14008R) supported by the Scientific Research for the High Level Talent of Xiamen University of Technology, China
Received date: 2014−04−11; **Accepted date:** 2014−09−15
Corresponding author: LUO Shan-ming, Professor, PhD; Tel: +86−592−6291386; E-mail: s.luo@hotmail.com

which coincides with the origin O_0. The line of action passes through the centrode point O_0. In coordinate system Σ_0, assume that the equation of the line of action can be expressed as

$$\begin{cases} x_0 = x_0(\theta) \\ y_0 = y_0(\theta) \end{cases} \tag{1}$$

where θ is the parameter of the line of action.

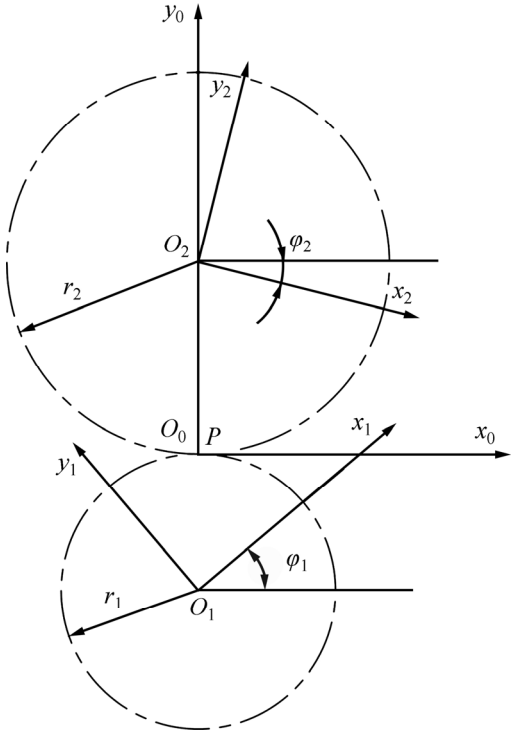

Fig. 1 Applied coordinate systems of meshing spur gears

According to Ref. [14], the equation of tooth profile of the driving gear, represented in coordinate system Σ_1, can be written as

$$\boldsymbol{\rho}_1 = \begin{bmatrix} \cos\varphi_1(\theta) & \sin\varphi_1(\theta) & r_1\sin\varphi_1(\theta) \\ -\sin\varphi_1(\theta) & \cos\varphi_1(\theta) & r_1\cos\varphi_1(\theta) \\ 0 & 0 & 1 \end{bmatrix} \begin{bmatrix} x_0 \\ y_0 \\ 1 \end{bmatrix} \tag{2}$$

where $\boldsymbol{\rho}_1$ denotes the position vector of contact point in coordinate system Σ_1.

By applying the coordinate transformations, the equation of the driven gear, represented in coordinate system Σ_2, can be expressed as [14]

$$\boldsymbol{\rho}_2 = \begin{bmatrix} [r_2 - y_0(\theta)]\sin\dfrac{\varphi_1(\theta)}{u} + x_0(\theta)\cos\dfrac{\varphi_1(\theta)}{u} \\ [y_0(\theta) - r_2]\cos\dfrac{\varphi_1(\theta)}{u} + x_0(\theta)\sin\dfrac{\varphi_1(\theta)}{u} \\ 1 \end{bmatrix} \tag{3}$$

where $\boldsymbol{\rho}_2$ denotes the position vector of contact point in coordinate system Σ_2 and u represents the contact ratio.

The meshing equation represents the necessary condition of existence of the envelope to a family of surface. The meshing equation can be deduced to [14]

$$\frac{r_1 x_0(\theta)\varphi_1'(\theta)}{\sqrt{[x_0(\theta)]^2 + [y_0(\theta)]^2}} \cdot \frac{\mathrm{d}\theta}{\mathrm{d}t} + \frac{x_0(\theta)x_0'(\theta) + y_0(\theta)y_0'(\theta)}{\sqrt{[x_0(\theta)]^2 + [y_0(\theta)]^2}} \cdot \frac{\mathrm{d}\theta}{\mathrm{d}t} = 0 \tag{4}$$

where $x_0'(\theta)$ and $y_0'(\theta)$ are the derivatives of $x_0(\theta)$ and $y_0(\theta)$ with respect to θ, respectively; $\varphi_1'(\theta)$ is the derivative of φ_1 with respect to θ, which can be obtained from Eq. (4) as follows:

$$\varphi_1 = -\frac{(1+u)}{a}\int_0^{\theta}\left[x_0'(\theta) + \frac{y_0(\theta)y_0'(\theta)}{x_0(\theta)}\right]\mathrm{d}\theta \tag{5}$$

where a represents the distance between the original points O_1 and O_2.

Substituting Eq. (5) into Eqs. (2) and (3), the equations of tooth profiles can be obtained.

According to the theory of gearing, undercutting occurs when the sliding velocity of contact point on the tooth profile is equal to zero at singular points [15]. According to Ref. [14], the conditions of undercutting of tooth profile of the drive and the driven gear can be derived as follows, respectively.

$$(1+u)x_0(\theta)x_0'(\theta) + [a + (1+u)y_0(\theta)]y_0'(\theta) = 0 \tag{6}$$

$$(1+u)x_0(\theta)x_0'(\theta) + y_0(\theta)y_0'(\theta) + u[y_0(\theta) - a] = 0 \tag{7}$$

3 Mathematical model of spur gears using elliptical segments as line of action

In this section, the mathematical model of tooth profiles using elliptical segments as its line of action is proposed. First of all, we look at a quarter section of an ellipse curve which is assumed to act as the line of action in the first quadrant. As shown in Fig. 2, the parameter θ is the angle between the line $O'B$ and axis y_0. Let A be the point of intersection of the line $O'B$ and the circle whose radius is b_1. In addition, making two perpendiculars from points A and O' to BN, respectively, the path of the point M is an ellipse curve. Supposing that a_1 and b_1 are the major and minor axes, the equation of the ellipse can be obtained.

$$\begin{cases} x_0 = a_1\sin\theta, \\ y_0 = b_1(1-\cos\theta), \end{cases} \quad 0 < \theta < \frac{\pi}{2}, 0 < b_1 < a_1 \tag{8}$$

Supposing that k_1 is the ratio of b_1 to r_2, the following equation exists:

$$b_1 = k_1 r_2 \tag{9}$$

where r_2 is the radius of the pitch circle of the driven gear.

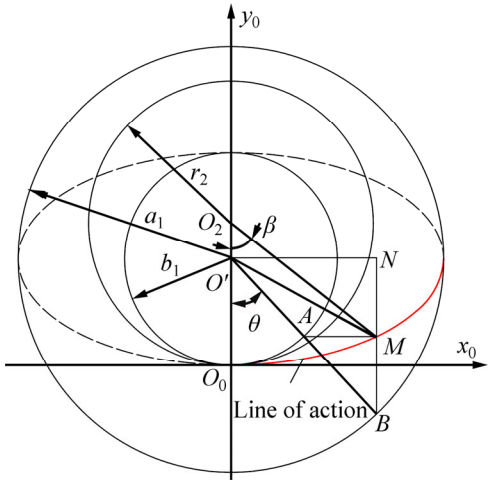

Fig. 2 Ellipse curve at first quadrant

Substituting Eqs. (8) and (9) into Eq. (4) gives

$$\frac{a_1^2 \sin\theta\cos\theta + b_1^2 \sin\theta(1-\cos\theta)}{\sqrt{[a_1\sin\theta]^2 + [b_1(1-\cos\theta)]^2}} + \frac{r_1 a_1 \sin\theta\varphi_1'(\theta)}{\sqrt{[a_1\sin\theta]^2 + [b_1(1-\cos\theta)]^2}} = 0 \tag{10}$$

From Eq. (10), we have

$$\varphi_1'(\theta) = -\frac{b_1^2}{r_1 a_1} - \frac{(a_1^2 - b_1^2)}{r_1 a_1}\cos\theta \tag{11}$$

By integrating Eq. (11) and substituting it into Eqs. (2) and (3), the equations of tooth profiles of the driving gear and the driven gear can be represented as

$$\begin{cases} x_1 = r_1 \sin\varphi_1(\theta) + a_1 \sin\theta\cos\varphi_1(\theta) + \\ \quad b_1(1-\cos\theta)\sin\varphi_1(\theta) \\ y_1 = r_1\cos\varphi_1(\theta) - a_1\sin\theta\sin\varphi_1(\theta) + \\ \quad b_1(1-\cos\theta)\cos\varphi_1(\theta) \end{cases} \tag{12}$$

$$\begin{cases} x_2 = r_2 \sin\left[\dfrac{\varphi_1(\theta)}{u}\right] + a_1\sin\theta\cos\left[\dfrac{\varphi_1(\theta)}{u}\right] - \\ \quad b_1(1-\cos\theta)\sin\left[\dfrac{\varphi_1(\theta)}{u}\right] \\ y_2 = -r_2\cos\left[\dfrac{\varphi_1(\theta)}{u}\right] + a_1\sin\theta\sin\left[\dfrac{\varphi_1(\theta)}{u}\right] + \\ \quad b_1(1-\cos\theta)\cos\left[\dfrac{\varphi_1(\theta)}{u}\right] \end{cases} \tag{13}$$

As the gears turn and the contact point moves to the third quadrant, we now study the driven gear and another ellipse. Similarly, as shown in Fig. 3, supposing that a_2 and b_2 are the major and minor axes, the equation of the ellipse can be defined by

$$\begin{cases} x_0 = -a_2\sin\theta, \\ y_0 = -b_2(1-\cos\theta), \end{cases} \quad 0 < \theta < \frac{\pi}{2}, 0 < b_2 < a_2 \tag{14}$$

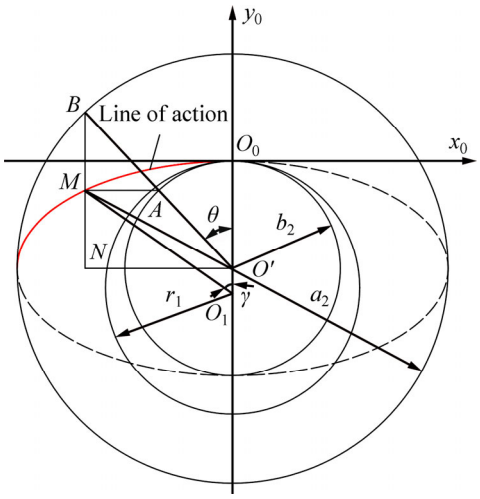

Fig. 3 Ellipse curve at third quadrant

Supposing that k_2 is the ratio of b_2 to r_1, we then have the following equation.

$$b_2 = k_2 r_1 \tag{15}$$

where r_1 denotes the radius of the pitch circle of the driving gear.

By the same method, the meshing equation can be deduced as

$$\frac{a_2^2 \sin\theta\cos\theta + b_2^2 \sin\theta(1-\cos\theta)}{\sqrt{[a_2\sin\theta]^2 + [b_2(1-\cos\theta)]^2}} - \frac{r_1 a_2 \sin\theta\varphi(\theta)}{\sqrt{[a_2\sin\theta]^2 + [b_2(1-\cos\theta)]^2}} = 0 \tag{16}$$

From Eq. (16) we have

$$\varphi_1'(\theta) = \frac{b_2^2}{r_1 a_2} + \frac{(a_2^2 - b_2^2)}{r_1 a_2}\cos\theta \tag{17}$$

By integrating Eq. (17) and substituting it into Eqs. (2) and (3), the equations of tooth profiles of the driving gear and the driven gear can be expressed respectively as

$$\begin{cases} x_1 = r_1\sin\varphi_1(\theta) - a_2\sin\theta\cos\varphi_1(\theta) - \\ \quad b_2(1-\cos\theta)\sin\varphi_1(\theta) \\ y_1 = r_1\cos\varphi_1(\theta) + a_2\sin\theta\sin\varphi_1(\theta) - \\ \quad b_2(1-\cos\theta)\cos\varphi_1(\theta) \end{cases} \tag{18}$$

$$\begin{cases} x_2 = b_2(1-\cos\theta)\sin\left[\dfrac{\varphi_1(\theta)}{u}\right] + \\ \quad r_2\sin\left[\dfrac{\varphi_1(\theta)}{u}\right] - a_2\sin\theta\cos\left[\dfrac{\varphi_1(\theta)}{u}\right] \\ y_2 = b_2(1-\cos\theta)\cos\left[\dfrac{\varphi_1(\theta)}{u}\right] - \\ \quad r_2\cos\left[\dfrac{\varphi_1(\theta)}{u}\right] - a_2\sin\theta\sin\left[\dfrac{\varphi_1(\theta)}{u}\right] \end{cases} \tag{19}$$

From what has been discussed above, the following conclusions can be made.

1) When the ellipse curve lies in the first quadrant, the corresponding tooth profile equations are Eqs. (12) and (13). Equation (12) represents the equation of tooth profile between pitch circle and addendum circle of the driving gear; while Eq. (13) denotes the equation of tooth profile between pitch circle and dedendum circle of the driven gear.

2) When the ellipse curve lies in the third quadrant, the corresponding tooth profile equations are Eqs. (18) and (19). Equation (18) represents the equation of tooth profile between pitch circle and dedendum circle of the driving gear; while Eq. (19) denotes the equation of tooth profile between pitch circle and addendum circle of the driven gear.

3) For the simplicity of discussion, let $a_1=k_3b_1=k_3k_1r_2$ ($k_3>1$) and $a_2=k_4b_2=k_4k_2r_1$ ($k_4>1$), the shape of the tooth profile above/below the pitch circle for the driving and below/above the pitch circle for the driven gear is only relevant to the parameters of the corresponding ellipse. This property allows the designer more easily to balance the thickness of the addendum and the thickness of the dedendum between the driving and driven gears. Therefore, the kinematic properties of a gear drive can be designed in a more controlled manor.

Substituting $a_1=k_3b_1$, $b_1=k_1r_2$ and Eq. (8) into Eq. (7), the critical condition of undercutting of tooth profile of the driven gear can be given as

$$\theta=\cos^{-1}\frac{1-k_1}{k_1(k_3^2-1)} \tag{20}$$

According to the gear meshing theory, the contact ratio should be greater than 1 in a gear drive for smooth transmission. When the contact point is located in the first quadrant as shown in Fig. 2, the angle β should be greater than the angle corresponding to a quarter of a tooth of the driven gear. The range of the angle β can be expressed as

$$\frac{\pi}{2uz_1}<\beta \tag{21}$$

According to Fig. 2, the following equation can be obtained.

$$\cos\beta=\frac{|O'O_2|^2+|MO_2|^2-|MO'|^2}{2|O'O_2||MO_2|} \tag{22}$$

where $|O'O_2|=r_2-b_1$, $|MO'|=\sqrt{x_0^2+(y_0-b_1)^2}$, $|MO_2|=\sqrt{x_0^2+(y_0-r_2)^2}$.

Substituting $a_1=k_3b_1$, $b_1=k_1r_2$ and Eq. (8) into Eq. (22) yields

$$\cos\beta=\frac{(1-k_1)\sqrt{k_3(k_3-1)(k_1^2k_3-2k_1+1)}}{(k_3-1)(k_1^2k_3-2k_1+1)} \tag{23}$$

According to Eqs. (20), (21) and (23), the ranges of the parameters k_1 and k_3 without undercutting and interference can be yielded.

$$\begin{cases}\dfrac{(1-k_1)\sqrt{k_3(k_3-1)(k_1^2k_3-2k_1+1)}}{(k_3-1)(k_1^2k_3-2k_1+1)}<\cos\left(\dfrac{\pi}{2uz_1}\right)\\ 0<\dfrac{1-k_1}{k_1(k_3^2-1)}<1\end{cases} \tag{24}$$

From Eq. (24), the range of the parameters k_1 and k_3 without undercutting and interference is shown in Fig. 4. The basic design space of the parameters k_1 and k_3 is enclosed by two dashed lines and a solid curve, whose equations can be expressed as

Line 1: $k_1=1$

Line 2: $k_3=1$

Curve 1: $$\frac{(1-k_1)\sqrt{k_3(k_3-1)(k_1^2k_3-2k_1+1)}}{(k_3-1)(k_1^2k_3-2k_1+1)}-\cos\left(\frac{\pi}{2uz_1}\right)=0 \tag{25}$$

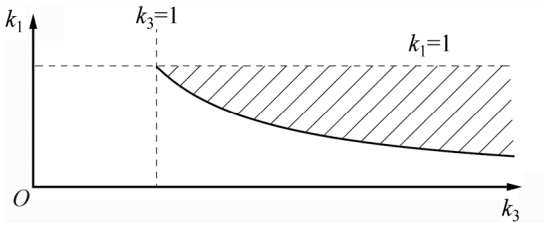

Fig. 4 Feasible ranges of parameters k_1 and k_3

Similarly, substituting $a_2=k_4b_2$, $b_2=k_2r_1$ and Eq. (14) into Eq. (6), the critical condition of undercutting of tooth profile of the driving gear can be obtained as

$$\theta=\cos^{-1}\frac{1-k_2}{k_2(k_4^2-1)} \tag{26}$$

When the contact point is in the third quadrant as shown in Fig. 3, the angle γ should be greater than the angle corresponding to a quarter of a tooth of the driving gear. By the same method, the range of the parameters k_2 and k_4 without undercutting and interference can be given as

$$\begin{cases}\dfrac{(1-k_2)\sqrt{k_4(k_4-1)(k_2^2k_4-2k_2+1)}}{(k_4-1)(k_2^2k_4-2k_2+1)}<\cos\left(\dfrac{\pi}{2z_1}\right)\\ 0<\dfrac{1-k_2}{k_2(k_4^2-1)}<1\end{cases} \tag{27}$$

As shown in Fig. 5, the basic design space of the parameters k_2 and k_4 is enclosed by two dashed lines and a solid curve, whose equations can be expressed as

Line 1: $k_2=1$

Line 2: $k_4=1$

$$\text{Curve 1: } \frac{(1-k_2)\sqrt{k_4(k_4-1)(k_2^2k_4-2k_2+1)}}{(k_4-1)(k_2^2k_4-2k_2+1)}-\cos\left(\frac{\pi}{2z_1}\right)=0 \tag{28}$$

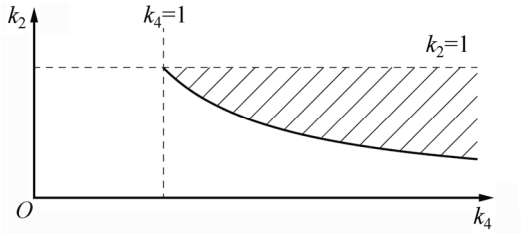

Fig. 5 Feasible range of parameters k_2 and k_4

4 Extended tooth profile from mathematical model

Specially, the line of action in the first quadrant will be a quarter section of a circle if the major axis a_1 is equal to the minor axis b_1, and Eq. (8) can be rewritten as

$$\begin{cases} x_0 = a_1\sin\theta, \\ y_0 = a_1(1-\cos\theta), \end{cases} \quad 0<\theta<\frac{\pi}{2} \tag{29}$$

By applying the similar process described in the previous section, the equations of tooth profiles of the driving gear and the driven gear can be represented as

$$\begin{cases} x_1 = (r_1+a_1)\sin\varphi_1(\theta)-a_1\sin[\varphi_1(\theta)-\theta] \\ y_1 = (r_1+a_1)\cos\varphi_1(\theta)-a_1\cos[\varphi_1(\theta)-\theta] \end{cases} \tag{30}$$

$$\begin{cases} x_2 = (r_2-a_1)\sin\dfrac{\varphi_1(\theta)}{u}+a_1\sin\left[\dfrac{\varphi_1(\theta)}{u}+\theta\right] \\ y_2 = -(r_2-a_1)\cos\dfrac{\varphi_1(\theta)}{u}-a_1\cos\left[\dfrac{\varphi_1(\theta)}{u}+\theta\right] \end{cases} \tag{31}$$

where $\varphi_1(\theta)$ can be solved from Eq. (11), and $\varphi_1(\theta)=-a_1\theta/r_1$.

Similarly, supposing that the major axis a_2 is equal to the minor axis b_2 in Eq. (14), the line of action in the third quadrant will also be a quarter section of a circle, which can be deduced as

$$\begin{cases} x_0 = -a_2\sin\theta, \\ y_0 = -a_2(1-\cos\theta), \end{cases} \quad 0<\theta<\frac{\pi}{2} \tag{32}$$

The equations of tooth profiles of the driving gear and the driven gear can be expressed respectively as

$$\begin{cases} x_1 = (r_1-a_2)\sin\varphi_1(\theta)+a_2\sin[\varphi_1(\theta)-\theta] \\ y_1 = (r_1-a_2)\cos\varphi_1(\theta)+a_2\cos[\varphi_1(\theta)-\theta] \end{cases} \tag{33}$$

$$\begin{cases} x_2 = (r_2+a_2)\sin\dfrac{\varphi_1(\theta)}{u}-a_2\sin\left[\dfrac{\varphi_1(\theta)}{u}+\theta\right] \\ y_2 = -(r_2+a_2)\cos\dfrac{\varphi_1(\theta)}{u}+a_2\cos\left[\dfrac{\varphi_1(\theta)}{u}+\theta\right] \end{cases} \tag{34}$$

where $\varphi_1(\theta)=\dfrac{a_2}{r_1}\theta$, which can be solved from Eq. (17).

From above discussion, the following conclusions to the proposed gears can be drawn.

1) Equations (30) and (33) represent the tooth profile above/below the pitch circle of the driving gear; while Eqs. (31) and (34) denote the tooth profile below/above the pitch circle of the driven gear, respectively. According to Ref. [5], tooth profiles of the driving and the driven gear are both epicycloidal. This coincides with the result of Ref. [13], which indicates that the line of action of cycloid gear drive is a circular arc.

2) The shape of the tooth profile above/below the pitch circle for the driving and below/above the pitch circle of the driven gear is only relevant to the parameters of the circle.

Substituting Eq. (29) into Eq. (7) and Eq. (32) into Eq. (6), the critical condition of undercutting of tooth profile of the driven and the driving gear can be respectively given as

$$a_1 = r_2 \tag{35}$$

$$a_2 = r_1 \tag{36}$$

5 Design example

According to the above-mentioned description, this study develops a computer simulation to plot the graphs for the gears, and investigate the tooth undercutting. An example gear drive is given to demonstrate the design process. The gears are designed to have a modulus of m=2 mm, a transmission ratio of u=1.2, an addendum coefficient of h_a^*=1, a bottom clearance of C^*=0.25, and a teeth number of z_1=15. The tooth fillet is the curve connecting the tooth profile and the root circle of a gear and generally by the tip of a rack or pinion cutter under generation cutting. For mold-made spur gears, the tooth fillet can be any curve. In this work, a circular arc is used as the tooth fillet.

This example develops a computer simulation of the tooth profile designed by the proposed method with the input parameter k_3=1.5 and k_4=1.8. According to Figs. 4 and 5, the ranges of parameters k_1 and k_2 without undercutting and interference were calculated to be $0.67<k_1<1$ and $0.56<k_2<1$, respectively. Here, parameters k_1 and k_2 were chosen as 0.7 and 0.8, respectively. The tooth profiles of the driving gear and the driven gear are established in Fig. 6 corresponding to above parameters. For the reason of comparison, the driving and the driven tooth profiles of the involute gear drive are also shown in Fig. 7. The pressure angle of the involute gear drive is α=20°; while the other parameters keep the same as the proposed gear drive. As shown in Fig. 7, in area of

addendum, the tooth thickness of proposed gear is greater than that of involute gear, but the tooth thickness shows the opposite trend in the part of dedendum.

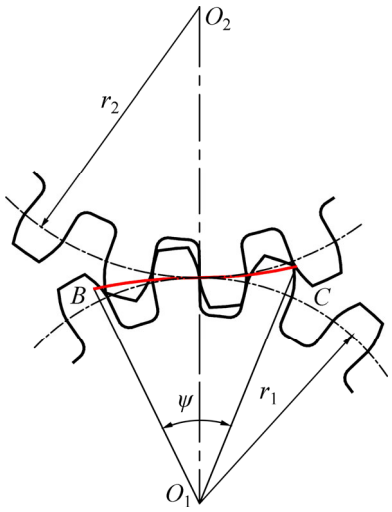

Fig. 6 Profiles using ellipse curve as its line of action

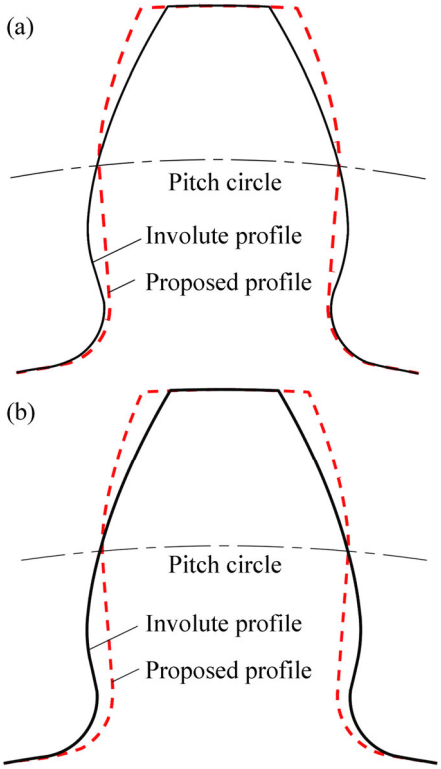

Fig. 7 Tooth profile using ellipse curve as its line of action: (a) Driving tooth profile; (b) Driven tooth profile

6 Evaluation of contact ratio

As illustrated in Fig. 8, B presents the intersection point between the line of action and the addendum circle of the driven gear and C is the intersection point between the line of action and the addendum circle of the driving gear. Assuming that the driving gear rotates in a clockwise direction, two gears would firstly engage at B, and finally separate at C. The contact ratio of the gear drive can be expressed as

$$\varepsilon = \frac{\psi}{2\pi/z_1} \tag{37}$$

where ψ denotes the angle between $\overline{O_1B}$ and $\overline{O_1C}$.

The parameters k_1, k_2, k_3 and k_4 are chosen as listed in Table 1 while the other parameters keep the same as in section 5. The contact ratios of the proposed gear drives are listed in Table 1. The contact ratio of the corresponding involute gear drive was also worked out for comparison.

From Table 1, the following conclusions to the specified gears can be drawn.

1) From Fig. 8, it can be seen that the greater the k_1, k_2, k_3 and k_4 are the larger the corresponding angle ψ will be. According to Eq. (37), the values of the contact ratio will increase with increased parameters k_1, k_2, k_3 and k_4. This has been confirmed by the results shown in Table 1.

2) The values of the contact ratio will increase; while one of the parameters k_1, k_2, k_3 and k_4 increases. Specially, the impact of parameters k_3 and k_4 on the contact ratio is greater than that of the parameters k_1 and k_2. Hence, the higher contact ratio will be obtained if parameters k_3 and k_4 increase suitably.

3) The contact ratio of the proposed gear drive varies from 2.0096 to 2.3013 in Table 1. The lowest value is nearly 25.1% higher than that of involute gear drive. According to Ref. [14], the contact ratio of the gear drive, using parabolic curve as its line of action, is nearly 10% less than that of involute gear drive. Therefore, the contact ratio of the proposed gear drive is much higher than that of the gear drive using parabolic curve as its line of action. This coincides with the result of Ref. [13], which indicates that the radius of curvature of the line of action will affect the contact ratio (i.e., the smaller the curvature of the line of action, the higher of the contact ratio of the corresponding gear drive).

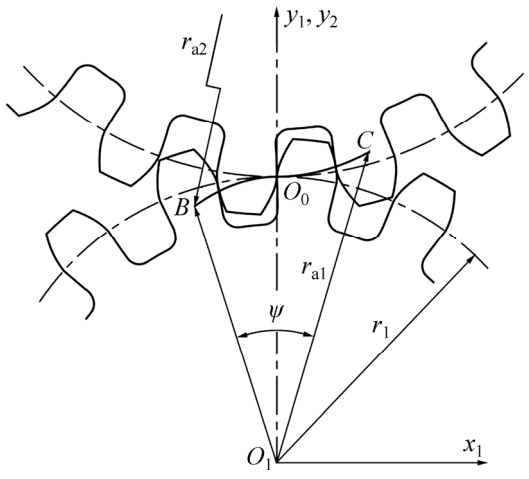

Fig. 8 Contact ratio of gear drive

Table 1 Contact ratio ε of gear drives under different parameters of k_1, k_2 , k_3 and k_4

Gear drive	Parameter				Contact ratio, ε
	k_1	k_2	k_3	k_4	
Proposed gear drive	0.7	0.7	1.5	1.8	2.0096
	0.8				2.0254
	0.9				2.0529
	0.7	0.8	1.5	1.8	2.0138
		0.9			2.0433
	0.7	0.7	1.8	1.8	2.0696
			2.5		2.1488
	0.9	0.9	2.5	1.8	2.2050
				2.5	2.2654
				3.5	2.3013
Involute gear drive	—	—	—	—	1.5050

7 Evaluation of tooth strength

In this section, an evaluation of the contact and bending stresses of the designed gears is made. The stress results presented in this work were obtained by using ANSYS, an FEA program. The parameters k_1, k_2, k_3 and k_4 are given in Table 2 and other parameters were set with the same values as those in section 5. The torque applied to the pinion was 105 N·m. Properties of materials were: μ = 0.29, E = 201 GPa. The involute gear drive used the same specifications for comparison.

The FEA model was constructed using 8-node isoparametric elements. Two options related to the contact problem, small sliding and no friction, have been selected. The bending stresses obtained in the fillet of the contacting tooth side were considered tension stresses, and those in the fillet of the opposite tooth side are considered compression stresses. The numerical results are listed in Table 2.

Table 2 Maximum bending and contact stresses

Gear type	k_1	k_2	k_3	k_4	Contact stress, σ_c/MPa	Bending stress (tension), σ_{bt}/MPa	Bending stress (compression), σ_{bc}/MPa
Proposed gear	0.7	0.7	1.5	1.8	411.63	166.20	205.92
	0.7	0.9	1.5	1.8	418.06	168.80	209.14
	0.7	0.7	1.8	1.8	407.34	164.47	203.78
Involute gear	—	—	—	—	510.50	190.23	246.93

From the obtained numerical results, the following conclusions can be made. The maximum contact stress of the proposed gear is reduced by 19.23% on average in comparison with the involute gear. The tension bending stress of the proposed gear is 12.48% on average less than that of the involute gear, and the compression bending stress is reduced by 16.46% on average in comparison with the involute gear. An application of the proposed tooth profile allows reducing both contact and bending stresses.

8 Conclusions

1) The shape of the tooth profile above/below the pitch circle for the driving and below/above the pitch circle of the driven gear is only relevant to the parameters of the corresponding elliptical segments. This property allows the designer more easily to balance the thickness of the addendum and the thickness of the dedendum between the driving and driven gears. Therefore, the kinematic properties and the strength of a gear drive can be designed in a more controlled manor.

2) The tooth profile designed by the proposed method will be an epicycloidal tooth profile when the line of action changed from an elliptical curve to a circle. The shape of the epicycloidal tooth profile is only relevant to the parameters of the circle.

3) The contact and the bending stresses of the designed gears are lower than those of the involute gears. In the case of example design, the contact ratio of the proposed gear drive varies from 2.0096 to 2.3013, which is much higher than that of the involute gear drive. It also indicates that the contact ratio of a spur gear drive can be controlled by specifying the values of the parameters for the line of action.

The related investigations on this gear drive, including the sensitivity to misalignments and other assembly errors, experiments of prototypes, and manufacturing method for mass production, are being carried out or would be the next step of work by the authors. Efforts putting this drive forward into practical application are also needed in the near future.

Acknowledgement

The authors also sincerely appreciate the comments and modification suggestions made by the editors and anonymous referees.

References

[1] LUO Shan-ming, WU Yue, WANG Jian. The generation principle and mathematical models of a novel gear drive [J]. Mechanism and Machine Theory, 2008, 43(12): 1543−1556.

[2] CHEN Xiao-xia, LIU Yu-sheng, XING Jing-zhong, LIN Shu-zhong, XU Wei. The parameter design of double-circular-arc tooth profile and its influence on the functional backlash of harmonic drive [J]. Mechanism and Machine Theory, 2014, 73(3): 1−24.

[3] FUENTES A, RUIZ-ORZAEZ R, GONZALEZ-PEREZ I. Computerized design, simulation of meshing, and finite element analysis of two types of geometry of curvilinear cylindrical gears [J]. Computer Methods in Applied Mechanics and Engineering, 2014,

272(15): 321−339.

[4] BAIR B W, SUNG M H, WANG J S, CHEN C F. Tooth profile generation and analysis of oval gears with circular-arc teeth [J]. Mechanism and Machine Theory, 2009, 44(6): 1306−1317.

[5] CHEN Bing-kui, ZHONG Hui, LIU Jing-ya, LI Chao-yang, FANG Ting-ting. Generation and investigation of a new cycloid drive with double contact [J]. Mechanism and Machine Theory, 2012, 49(3): 270−283.

[6] TSAI M H, TSAI Y C. Design of high-contact-ratio spur gear using quadratic parametric tooth profiles [J]. Mechanism and Machine Theory, 1998, 33(5): 551−564.

[7] WANG Jian, LUO Shan-ming, WU Yue. A method for the preliminary geometric design of gear tooth profiles with small sliding coefficients [J]. ASME, Journal of Mechanical Design, 2010, 132(5): 1−8.

[8] DANIELI G A, MUNDO D. New developments in variable radius gears using constant pressure angle teeth [J]. Mechanism and Machine Theory, 2005, 40(2): 203−217.

[9] WANG P Y, FONG Z H. Fourth-order kinematic synthesis for face-milling spiral bevel gears with modified radial motion (MRM) correction [J]. ASME Journal of Mechanical Design, 2006, 128(2): 457−467.

[10] LEE C K. Manufacturing process for a cylindrical crown gear drive with a controllable fourth order polynomial function of transmission error [J]. Journal of Materials Processing Technology, 2009, 209(1): 3−13.

[11] CAO Xue-mei, FANG Zong-de, XU Hao, SU Jin-zhan. Design of pinion machine tool-settings for spiral bevel gears by controlling contact path and transmission errors [J]. Chinese Journal of Aeronautics, 2008, 21(2): 179−186. (in Chinese)

[12] TSAI Y C, HSU W Y. The study on the design of spiral bevel gear sets with circular-arc contact paths and tooth profiles [J]. Mechanism and Machine Theory, 2008, 43(9): 1158−1174.

[13] FONG Z H, CHIANG T W, TSAI C W. Mathematical model for parametric tooth profile of spur gear using line of action [J]. Mathematical and Computer Modelling, 2002, 36 (4/5): 603−614.

[14] WANG Jian, HOU Liang, LUO Shan-ming, WU Yue. Active design of tooth profiles using parabolic curve as the line of action [J]. Mechanism and Machine Theory, 2013, 67(9): 47−63.

[15] LITVIN F L, FUENTES A. Gear geometry and applied theory [M]. 2nd ed. New York: Cambridge University Press, 2004.

(Edited by DENG Lü-xiang)